New Bleeding Model of Additives in a Polypropylene Film under Atmospheric Pressure

Makoto Wakabayashi,[1,2] Takayuki Kohno,[3] Tokutaro Kimura,[3] Satoshi Tamura,[3] Masahiko Endoh,[3] Satoru Ohnishi,[4] Toshikatsu Nishioka, Yoshikatsu Tanaka,[3] Toshitaka Kanai[1,2,3]

[1]*Central Research Laboratories, Idemitsu Kosan Co., 1-1 Anesakikaigan, Ichihara, Chiba 299-0193, Japan*
[2]*Division of Material Sciences, Graduate School of Natural Science and Technology, Kanazawa University, Kanazawa, Kakuma-Machi, Kanazawashi, Ishikawa 920–1192, Japan*
[3]*Prime Polymer Co., 580-30 Nagaura, Sodegaurashi, Chiba, 299-0265, Japan*
[4]*R&D Center for Plastic Products, Idemitsu Unitech Co., Ltd., 1660 Kamilzumi, Sodegaurashi, Chiba, 229-0205, Japan*

Received 11 June 2006; accepted 3 November 2006
DOI 10.1002/app.25922
Published online in Wiley InterScience (www.interscience.wiley.com).

ABSTRACT: Many additives are commercially used to add more favorable qualities to films. The bleeding process by which the additive in a film comes to the surface is considered. A new bleeding model of additives in a polypropylene film under atmospheric pressure was investigated. Solubility and diffusion are found to be important for explaining this bleeding process. The solubilities and diffusion coefficients of higher fatty acid amides such as erucamide (13-*cis*-docosenamide) and behenamide (docosanamide) were determined between 40 and 70°C and the difference between the solubilities and the diffusion coefficients was discussed. The experimental results are explained more precisely by assuming two transport processes between the crystalline regions and the amorphous ones. © 2007 Wiley Periodicals, Inc. J Appl Polym Sci 104: 3751–3757, 2007

Key words: polypropylene; films; additives; solubility; diffusion

INTRODUCTION

Many additives are used to add more favorable qualities to films. There are some additives, such as a slip agent or an antistatic additive, etc., that provide performance by bleeding on the surface of the film. Also, there are other additives applied inside the film, for example, an antioxidant and a nucleating agent, etc. The bleeding process by which the additive in a film comes to the surface will be considered to be effective in design development of additive prescription, if it can be predicted. However, there is no clear explanation of the bleeding process of the additive under atmospheric pressure until now.

There are many reports regarding the solubilities and the diffusions of additives in polymer films.[1–12] To measure the diffusion coefficient and the solubility, the methods of using the permeation through a film, adsorption in a film, and release from a film have been devised.[13–16] It is reported that the bleeding process can be explained by the solubility and the migration speed of an additive in a film. However, it is thought that the diffusion is influenced by the difference in morphology such as a crystalline state and an amorphous state.

Quijada-Garrido and others reported the migration speed of the erucamide (13-*cis*-docosenamide) in an isotactic polypropylene (iPP) film under atmospheric pressure and vacuum.[17,18] Under atmospheric pressure, by using the diffusion cell techniques, they proposed a so-called semiempirical sorption model that was described as a linear superposition of phenomenologically independent contribution from two simultaneous Fickian diffusion processes. They assumed that erucamide diffusing within iPP may be present in two different sites. In vacuum, by using mechanical blending methods, they proposed two terms for the overall transport process containing a diffusion term that described in the amorphous regions of spherulites and a term that described the release from the globules to the amorphous regions of spherulites. They mentioned that crystallites and spherulites in an iPP film proceeded by cooling. The excess of erucamide forms independently as globules or droplets at a high concentration. The erucamide in the amorphous regions migrates on the film surface according to the above-mentioned theory, and is removed very rapidly.

It is still important that the morphology of an iPP film such as crystallites and spherulites are taken into consideration. But it seems that there is yet no satisfactory explanation of the bleeding process of the erucamide in an iPP film under atmospheric pressure.

Correspondence to: M. Wakabayashi (makoto.wakabayashi@si.idemitsu.co.jp).

Journal of Applied Polymer Science, Vol. 104, 3751–3757 (2007)
© 2007 Wiley Periodicals, Inc.
WILEY InterScience® DISCOVER SOMETHING GREAT

EXPERIMENTAL

Materials

Idemitsu H700 additive-free isotactic polypropylene (iPP) was used. It has a nominal density of 900 kg/m^3, MFR 7.0 g/10 min, 47% of crystallinity, and 93.2 mol % of isotactic pentad fraction evaluated by ^{13}C NMR spectroscopy; the average molecular masses of H700 are $M_n = 4.87 \times 10^4$, $M_w = 3.25 \times 10^5$, and $M_z = 1.31 \times 10^6$ estimated by size exclusion chromatography. Erucamide (13-*cis*-docosenamide) and behenamide (docosanamide) were supplied by NFC Co., Ltd. (Osaka, Japan).

Sample preparation and measurements

The blends of iPP/erucamide or iPP/behenamide with a small quantity of antioxidant additives (500 ppm of IRGANOX 1076 (Ciba-Geigy) and 500 ppm of IRGAFOS 168 (Ciba-Geigy)) were prepared by dry mixing and then fed into single-screw extruder operated at 200°C with a screw speed of 100 rpm. They were quenched in cold water and cut into the pellet form. The obtained pellets were fabricated into 50-μm-thick film using the Φ 40 mm T-die casting machine, wherein the temperature from the bottom of the hopper to the T-die was set from 200 to 230°C with a screw speed of 80 rpm. The film was chilled at 30°C. Several sets of 50 sheets of film whose area became 100 cm^2 (10 cm long and 10 cm wide) were prepared and were put in the oven quickly after fabrication for bleeding under the predetermined temperature and time.

A set of the 50 sheets of film was taken out from the oven after predetermined time. Each surface of 50 sheets of film was put in 500 mL ethanol for erucamide or 500 mL chloroform for behenamide for 5 s and then washed for 5 s. The solvents were eliminated by using rotary evaporator. The amounts of the slip agents were determined by Shimadzu GC-14A gas chromatograph.

RESULTS AND DISCUSSION

Diffusion model

The optimal model for describing the bleeding process under atmospheric pressure was examined. The bleeding process is thought to be governed by Fick's eqs. (1) with the appropriate boundary conditions.

$$\frac{\partial c}{\partial t} = D\,\frac{\partial^2 c}{\partial x^2} \tag{1}$$

where c is the concentration of diffusion material in any point x at time t, and D is the diffusion coefficient. The boundary conditions of Fick's equation, which assumed the diffusion in the object spread infinitely, were examined. The boundary conditions of this diffusion model are described below.

$$\begin{array}{lll} t = 0 & c = C_{0,i} - C_s & (-l < x < l) \\ & c = 0 & (x < -l,\ l < x) \end{array} \tag{2}$$

where l is the half thickness of the film, $C_{0,i}$ is the initial amount i of an additive, and C_s is the saturation solubility. The solution yields this expression:

$$C(x,t) = \frac{C_{0,i} - C_s}{2}\,c(x,t) \tag{3}$$

$$c(x,t) = \mathrm{erf}\left(\frac{l-x}{2\sqrt{Dt}}\right) + \mathrm{erf}\left(\frac{l+x}{2\sqrt{Dt}}\right) \tag{4}$$

where erf(x) is the error function described below.

$$erf(x) = \frac{1}{\sqrt{\pi}}\int_0^x \exp(-t^2)dt \tag{5}$$

Then the amount of bleeding additive on the film $y(t)$ is assumed to be the difference between the excess amount of additive ($C_{0,I} - C_s$) and the remaining amount of additive inside the film at time t.

$$y(t) = \left(C_{0,i} - C_s\right)\left(1 - \frac{1}{4l}\left(\int_{-l}^{l} c(x,t)dx\right)\right) \tag{6}$$

Figure 1 shows the concept for calculation of the bleeding process. The area outside of the film surface is assumed to be the amount of bleeding additive.

The saturation solubility and the diffusion coefficient were obtained from the bleeding experiment of erucamide at 40°C and behenamide at 50°C by using the above-mentioned diffusion model. Values are calculated by the least squares technique using a computer program. The values of saturation solubilities (C_s) of erucamide and behenamide are calculated with 200 ppm and 0 ppm respectively. And the values of the diffusion coefficients (D) of erucamide and behenamide were calculated with 2.1×10^{-15} and 4.6×10^{-16} m^2/s respectively. The result calculated using the saturation solubility and the diffusion coefficient of erucamide is shown in Figure 2. It turns out that the diffusion model which assumed the diffusion in the object spread infinitely is in agreement with an actual measurement to some extent. This shows that the diffusion of erucamide in an iPP film under atmospheric pressure almost follows the model which assumed the diffusion in the object spread infinitely. But it turns out that there is a slight gap between the experimental values and the calculated ones. The result of behenamide is shown in Figure 3. It turns out that there is a large gap between the experimental values and the calculated ones. It is concluded that this model could not explain the bleeding process completely.

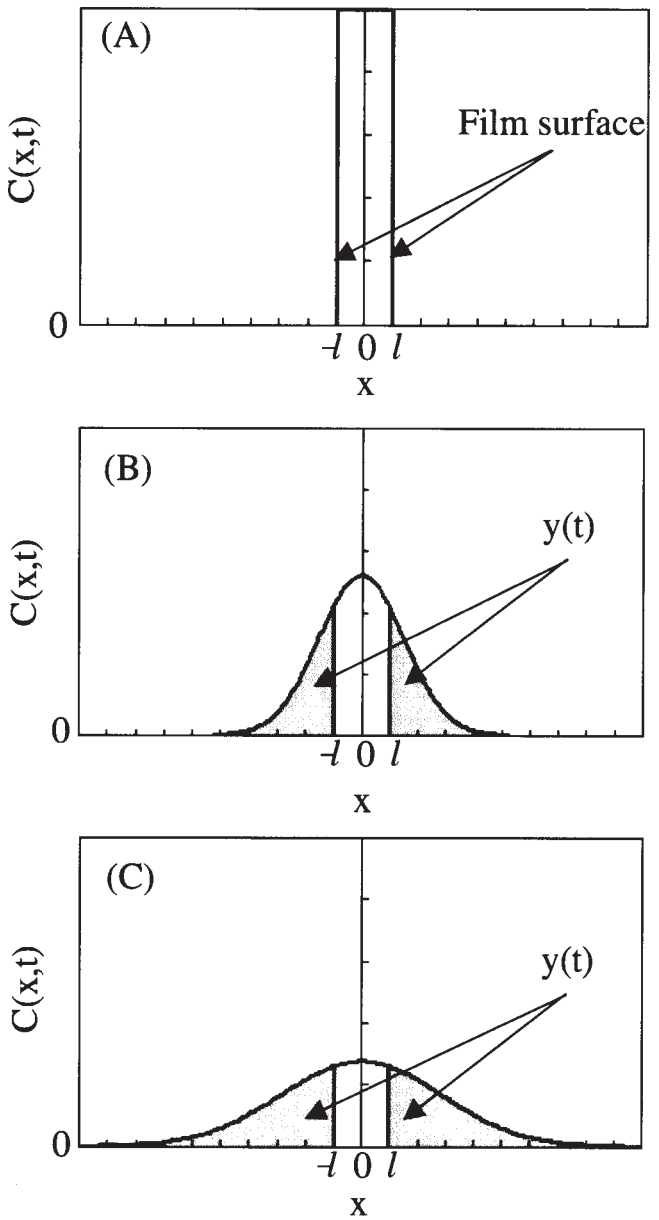

Figure 1 Concept for calculation of bleeding process assuming the diffusion in the object spread infinitely. (A) $t = 0$, (B) $t = 1/D$, (C) $t = 4/D$.

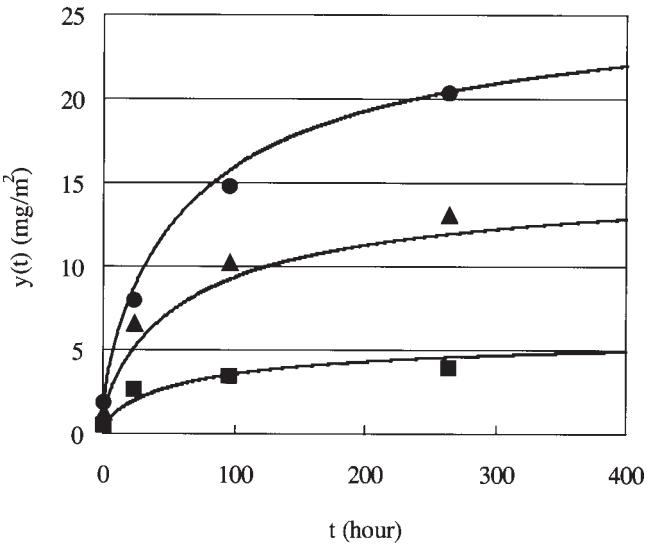

Figure 2 Bleeding profiles of erucamide (13-*cis*-docosenamide) at 40°C. Initial amount ($C_{0,i}$): $C_{0,1}$ = 500 ppm (■); $C_{0,2}$ = 1000 ppm (▲); $C_{0,3}$ = 1500 ppm (●). The full lines were calculated by using the diffusion model assuming the diffusion in the object spread infinitely.

Modified model

Quijada-Garrido and others had reported about the erucamide in iPP film.[17–22] Under vacuum at a high concentration the erucamide passes through the amorphous regions according to a diffusion equation and is released from the globules to the amorphous regions according to first-order kinetics. Then, the amount of desorption of the erucamide is described as the sum of two processes. We considered the bleeding process of the additives under atmospheric pressure as follows. The additive in an iPP film dissolves in an amorphous region first, and if it reaches saturation solubility it becomes impossible to dissolve more. The ingredient beyond this saturation solubility migrates to the film surface at a certain speed according to the diffusion process. Furthermore, as shown in Figure 4, it is known that an iPP film has spherulites (S) and amorphous regions (A), which are supposed to have a different contribution to the migration speed in the bleeding process. The spherulites have folded crystalline regions (C) and the additives exist among the crystalline regions (A′). So the model had to be modified in consideration of

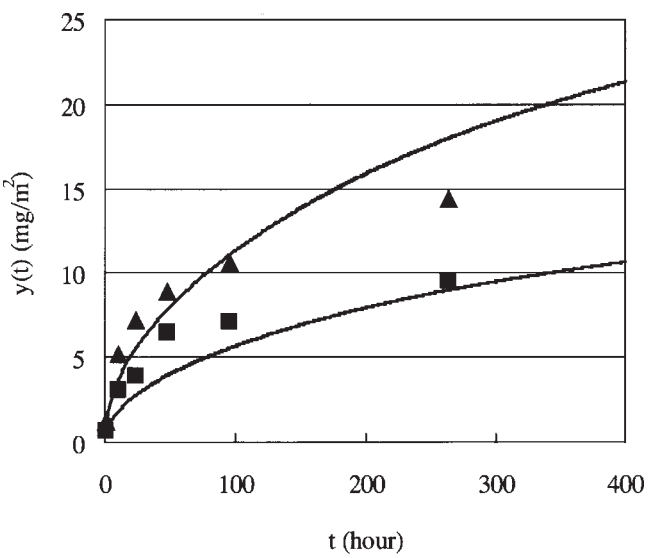

Figure 3 Bleeding profiles of behenamide (docosanamide) at 50°C. Initial amount ($C_{0,i}$): $C_{0,1}$ = 1000 ppm (■); $C_{0,2}$ = 2000 ppm (▲). The full lines were calculated by using the diffusion model assuming the diffusion in the object spread infinitely.

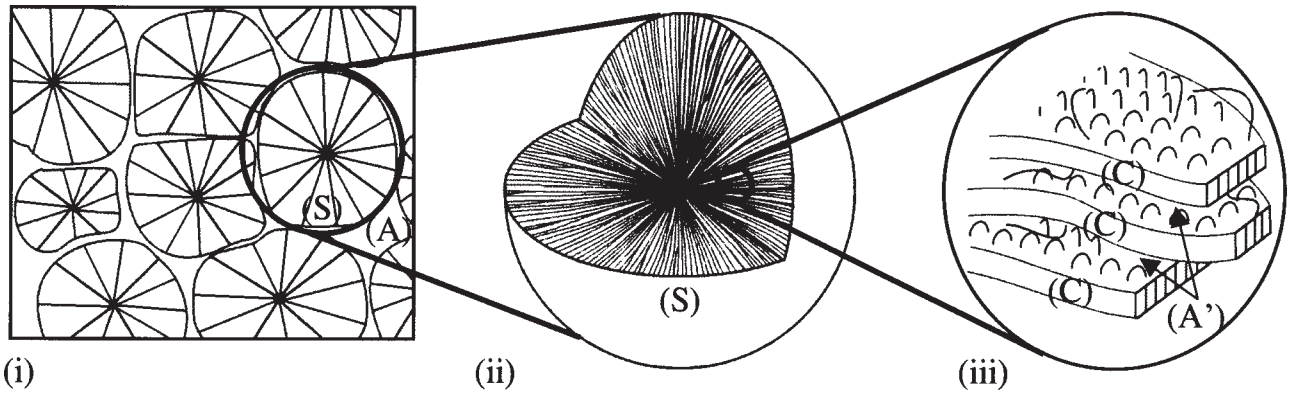

Figure 4 Internal structure of isotactic polypropylene[23–26]: (i) spherulites (S) and amorphous regions (A) among spherulites in iPP film; (ii) internal structure of a spherulite (S); (iii) the chain folded crystalline regions (C) and amorphous regions (A′) among the chain folded crystalline regions.

the amorphous regions and the crystalline regions. We considered that a portion of the excess amount beyond the saturation solubility was restricted within crystalline regions in the spherulites and migrated slowly according to the first-order kinetics. The rest of the excess amount of additives which is not restricted in the crystalline regions exists in the amorphous regions among spherulites. The extent of restriction within crystalline regions was assumed to increase according to the initial amount of the additives. So modified model yields the expression

$$y(t) = (C_{0,i} - C_s)\{\alpha_i + (1 - \alpha_i) \times (1 - \exp(-kt))\}\left(1 - \frac{1}{4l}\left(\int_{-l}^{l} c(x,t)dx\right)\right) \quad (7)$$

$$c(x,t) = \mathrm{erf}\left(\frac{l-x}{2\sqrt{Dt}}\right) + \mathrm{erf}\left(\frac{l+x}{2\sqrt{Dt}}\right) \quad (8)$$

where $y(t)$ is the amount of bleeding additive on the film surface at time t, $C_{0,i}$ is the initial amount i of an additive, C_s is the saturation solubility, α_i is a diffusion ratio of the initial amount $C_{0,i}$, k is the constant of first-order kinetics, l is the half thickness of film, $c(x, t)$ is the concentration at time t and distance x, erf(z) is the error function, and D is the diffusion coefficient.

The diffusion ratio α_i is assumed to be larger at a lower concentration of additive, because the restriction within the crystalline regions of spherulites is thought to be weak at a lower concentration. Values are calculated by the least squares technique using a computer program.

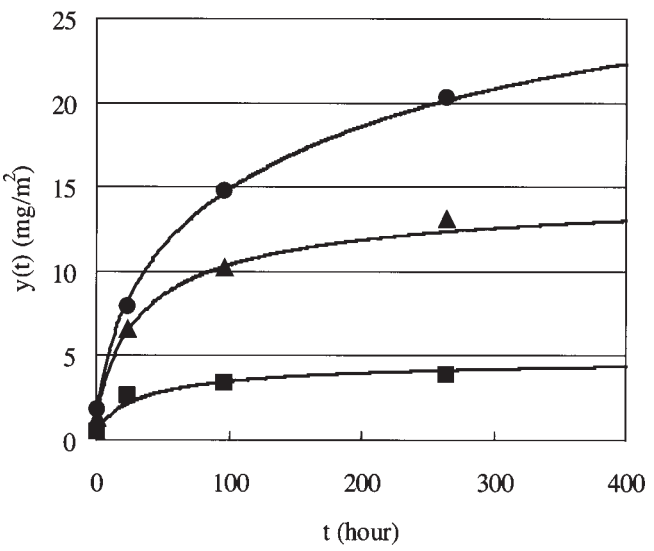

Figure 5 Bleeding profiles of erucamide (13-*cis*-docosenamide) at 40°C. Initial amount ($C_{0,i}$): $C_{0,1}$ = 500 ppm (■); $C_{0,2}$ = 1000 ppm (▲); $C_{0,3}$ = 1500 ppm (●). The full lines were calculated by using the modified model.

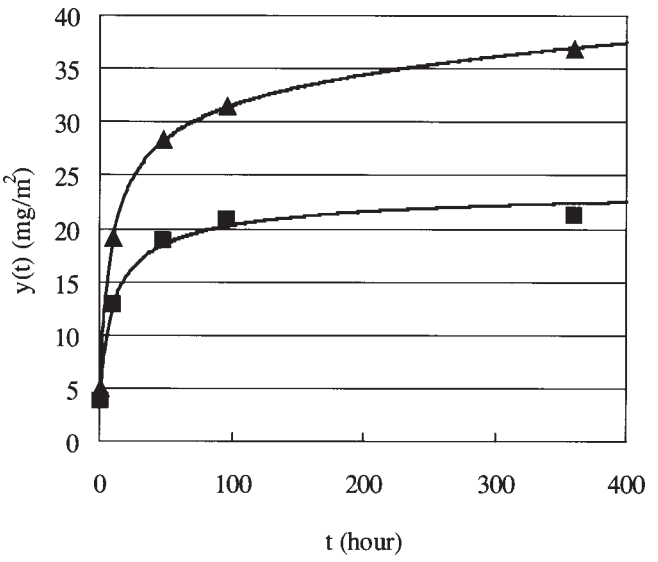

Figure 6 Bleeding profiles of erucamide (13-*cis*-docosenamide) at 50°C. Initial amount ($C_{0,i}$): $C_{0,1}$ = 3000 ppm (■); $C_{0,2}$ = 4000 ppm (▲). The full lines were calculated by using the modified model.

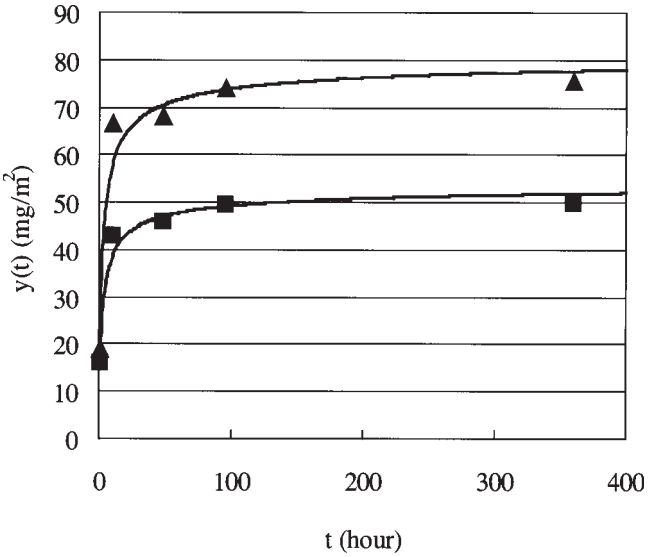

Figure 7 Bleeding profiles of erucamide (13-*cis*-docosenamide) at 60°C. Initial amount ($C_{0,i}$): $C_{0,1}$ = 6000 ppm (■); $C_{0,2}$ = 8000 ppm (▲). The full lines were calculated by using the modified model.

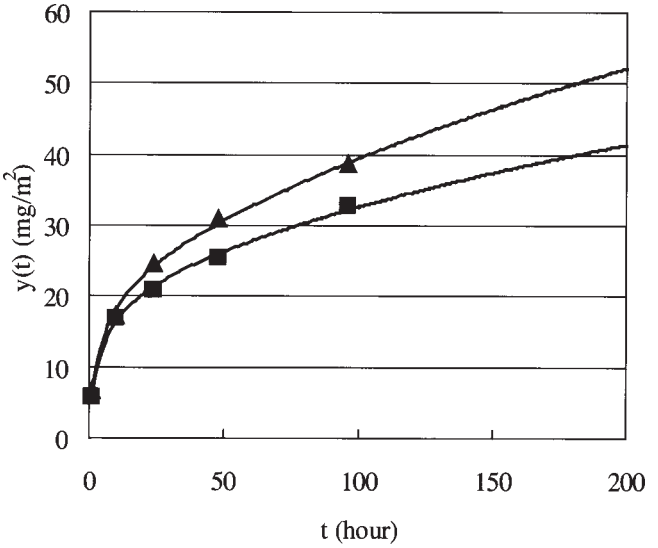

Figure 9 Bleeding profiles of behenamide (docosanamide) at 60°C. Initial amount ($C_{0,i}$): $C_{0,1}$ = 3000 ppm (■); $C_{0,2}$ = 4000 ppm (▲). The full lines were calculated by using the modified model.

The result of erucamide at 40°C calculated using the modified model is shown in Figure 5. By comparing with Figure 2, the modified model explains the bleeding profiles better than the diffusion model. The results of erucamide at 50 and 60°C are shown in Figures 6 and 7 respectively. The modified model explains the bleeding profiles of erucamide well.

Behenamide (docosanamide) is also used as a slip agent. It is known empirically that when compared with erucamide, behenamide demonstrates the slipping performance at a higher temperature but begins to demonstrate slipping performance more slowly. The experimental plots and calculated lines of behenamide at 50, 60, and 70°C are shown in Figures 8, 9, and 10 respectively. The modified model also explains the bleeding profiles of behenamide well.

Table I presents the saturation solubilities, the diffusion coefficients, the constants of first-order

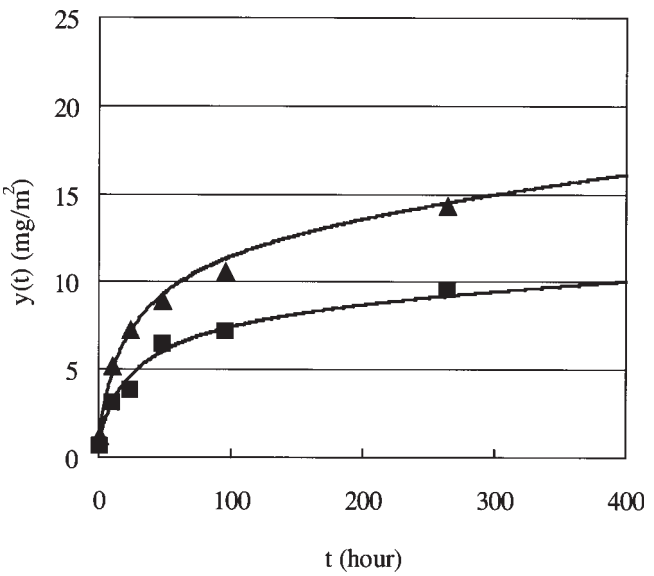

Figure 8 Bleeding profiles of behenamide (docosanamide) at 50°C. Initial amount ($C_{0,i}$): $C_{0,1}$ = 1000 ppm (■); $C_{0,2}$ = 2000 ppm (▲). The full lines were calculated by using the modified model.

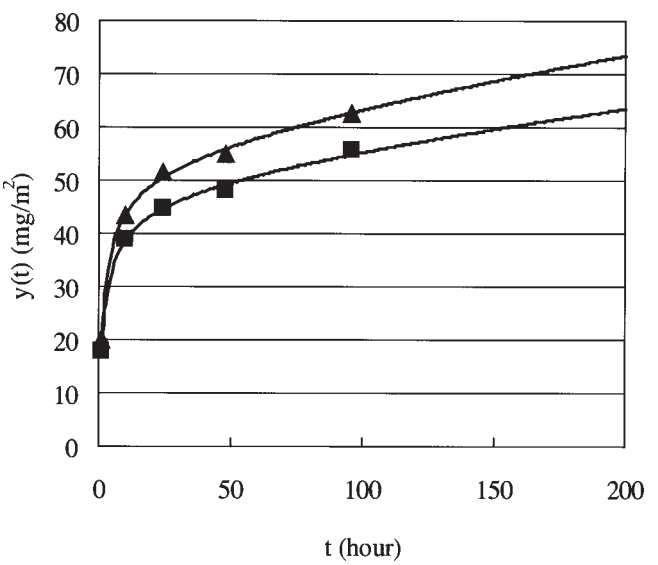

Figure 10 Bleeding profiles of behenamide (docosanamide) at 70°C. Initial amount ($C_{0,i}$): $C_{0,1}$ = 5000 ppm (■); $C_{0,2}$ = 6000 ppm (▲). The full lines were calculated by using the modified model.

TABLE I
Parameters Determined by the Modified Model

Additive	Temperature (°C)	Saturation solubility, C_s (ppm)	Diffusion coefficient, D (m^2/s)	Constant of first-order kinetics, k (1/s)	Diffusion ratio		
					α_1	α_2	α_3
Erucamide	40	250	5.2×10^{-15}	1.6×10^{-6}	0.96[a]	0.92[a]	0.58[a]
	50	1900	1.6×10^{-14}	3.3×10^{-7}	1.00[b]	0.79[b]	
	60	3600	5.7×10^{-14}	0	0.99[c]	0.82[c]	
Behenamide	50	0	4.5×10^{-15}	8.7×10^{-8}	0.48[d]	0.35[d]	
	60	0	2.3×10^{-14}	8.9×10^{-7}	0.41[e]	0.33[e]	
	70	0	6.4×10^{-14}	4.2×10^{-7}	0.47[f]	0.44[f]	

The initial amounts of additives ($C_{0,i}$).
[a] $C_{0,1}$: 500 ppm, $C_{0,2}$: 1000 ppm, $C_{0,3}$: 1500 ppm.
[b] $C_{0,1}$: 3000 ppm, $C_{0,2}$: 4000 ppm.
[c] $C_{0,1}$: 6000 ppm, $C_{0,2}$: 8000 ppm.
[d] $C_{0,1}$: 1000 ppm, $C_{0,2}$: 2000 ppm.
[e] $C_{0,1}$: 3000 ppm, $C_{0,2}$: 4000 ppm.
[f] $C_{0,1}$: 5000 ppm, $C_{0,2}$: 6000 ppm.

kinetics, and the diffusion ratios of erucamide and behenamide based on the modified model. The saturation solubility of erucamide increased with increasing the temperature, but the saturation solubility of behenamide is maintained zero at 50, 60, and 70°C. Since the saturation solubility of behenamide is maintained zero as temperature rises, the slipping performance of behenamide is still thought to be demonstrated at a higher temperature. On the other hand, since the saturation solubility of erucamide increases and the ingredient beyond the saturation solubility decreases to zero as temperature rises, the slipping performance of erucamide is thought to be lost at a higher temperature. Figure 11 presents the Arrhenius plot of the diffusion coefficients of erucamide and behenamide. The migration speed of erucamide is faster than that of behenamide. This shows that erucamide can bleed on the film surface faster and demonstrates slipping performance more rapidly. For this reason, behenamide demonstrates slipping performance more slowly.

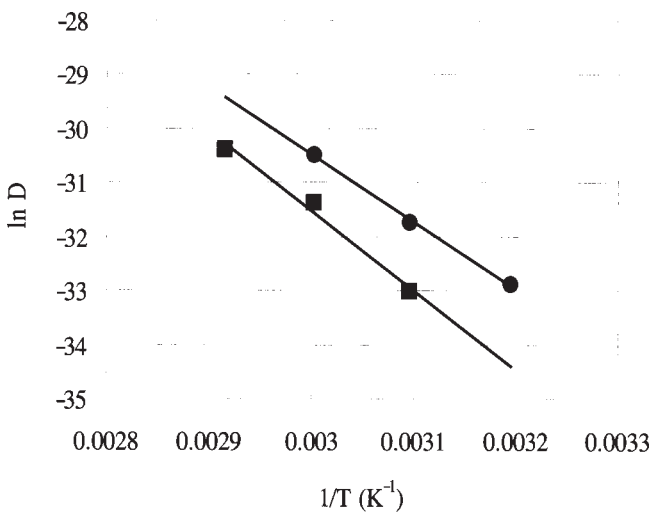

Figure 11 Arrhenius plot as ln D against $1/T$ for erucamide and behenamide in the iPP film. Erucamide (●); behenamide (■).

The diffusion ratios of erucamide are larger than 0.79. This means the diffusion is dominant to the bleeding process of erucamide. On the other hand, the diffusion ratios of behenamide are between 0.33 and 0.48 in this experiment. This means behenamide easily becomes restricted in the crystalline regions in the spherulites because the diffusion of behenamide is slower than that of erucamide.

Temperature dependence of the diffusion coefficient

As shown in Figure 11, it turned out that both diffusion coefficients follow the Arrhenius rule.

$$D = D_0 \exp\left(\frac{-E_d}{RT}\right) \tag{9}$$

where E_d is the activation energy, D_0 is the preexponential factor, R is the gas constant, and T is the temperature.

The values of the activation energies (E_d) and preexponential factors (ln D_0) are given in Table II. It is shown that the values of activation energy (E_d) and

TABLE II
Activation Energy and Preexponential Factors for Erucamide and Behenamide

Additive	Activation energy, E_d (kJ/mol)	Preexponential factor, ln D_0 (D_0 in m^2/s)
Erucamide	104	7.1
Behenamide	122	12.6

preexponential factor (ln D_0) of behenamide are larger than the values of erucamide. Möller and Gevert demonstrated that both E_d and ln D_0 of hindered phenols in LDPE increased linearly as molar mass of hindered phenols increased.[5] The molar mass of behenamide (MW, 340) is almost equal to the molar mass of erucamide (MW, 338). If the molecular size of behenamide were equal to that of erucamide, E_d and ln D_0 of behenamide and erucamide should become almost the same. However, since E_d and ln D_0 of behenamide are larger than those of erucamide, it is thought that the molecular size of behenamide is larger than the molecular size of erucamide. This is supported from the result that the saturation solubility of behenamide is smaller than the saturation solubility of erucamaide. Furthermore, because behenamide is more easily absorbed in the crystalline regions during the crystallization of iPP, it is thought that the diffusion ratio of behenamide is low. The reason why the molecular size of behenamide is larger than that of erucamide is thought to be because the self-association of behenamide occurs in iPP film.

CONCLUSIONS

A new bleeding model of additives in a polypropylene film under atmospheric pressure was investigated. Solubility and diffusion are found to be important for explaining this bleeding process. The solubilities and diffusion coefficients of higher fatty acid amides such as erucamide (13-*cis*-docosenamide) and behenamide (docosanamide) were determined between 40 and 70°C and the difference between the solubilities and the diffusion coefficients was discussed. It was found that the experimental results were explained more precisely by assuming two transport processes between the crystalline regions and the amorphous ones. The difference between the bleeding profiles of erucamide and behenamide can be explained by assuming that the self-association of behenamide occurs in iPP film.

References

1. Billingham, N. C.; Calvert, P. D.; Manke, A. S. J Appl Polym Sci 1981, 26, 3543.
2. Földes, E.; Turcsányi, B. J Appl Polym Sci 1992, 46, 507.
3. Földes, E. J Appl Polym Sci 1993, 1905, 48.
4. Földes, E. J Appl Polym Sci 1994, 51, 1581.
5. Möller, K.; Gevert, T. J Appl Polym Sci 1994, 51, 895.
6. Spatafore, R.; Pearson, L. T. Polym Eng Sci 1991, 31, 1610.
7. Schwarz, T.; Steiner, G.; Koppelmann, J. J Appl Polym Sci 1989, 37, 3335.
8. Koszinowski, J. J Appl Polym Sci 1986, 31, 2711.
9. Hayashi, H.; Sakai, H.; Matsuyama, S. J Appl Polym Sci 1994, 51, 2165.
10. Reynier, A.; Dole, A. P.; Humbel, S.; Feigenbaum, A. J Appl Polym Sci 2001, 82, 2422.
11. Reynier, A.; Dole, P.; Feigenbaum, A. J Appl Polym Sci 2001, 82, 2434.
12. Schuler, C. A.; Janorkar, A. V.; Hirt, D. E. Polym Eng Sci 2004, 44, 2247.
13. Billingham, N. C.; Calvert, P. D. In Developments in Polymer Stabilization; Scott, G., Ed.; Applied Science: London, 1980; Vol. 3, p 139.
14. Roe, R. J.; Bair, H. E.; Gieniewski, C. J. J Appl Polym Sci 1974, 12, 843.
15. Moisan, J. Y. In Polymer Permeability; Comyn, J., Ed.; Elsevier: London, 1985; p 119.
16. Crank, J. G.; Park, S. In Difusion in Polymers; Crank, J.; Park, G. S., Eds.; Academic Press: New York, 1968.
17. Quijada-Garrido, I.; Frutos, G.; Barrales-Rienda, J. M. Macromolecules 1996, 29, 7164.
18. Quijada-Garrido, I.; Barrales-Rienda, J. M.; Alejo Espinoza, L.; Fierro, J. L. G. Macromolecules 1996, 29, 8791.
19. Quijada-Garrido, I.; Barrales-Rienda, J. M.; Frutos, G.; Pereña, J. M. Polymer 1997, 38, 5125.
20. Quijada-Garrido, I.; Barrales-Rienda, J. M.; Pereña, J. M.; Frutos, G. J Polym Sci Part B: Polym Phys 1997, 35, 1473.
21. Quijada-Garrido, I.; Wilhelm, M.; Spiess, H. W.; Barrales-Rienda, J. M. Macromol Chem Phys 1998, 199, 985.
22. Quijada-Garrido, I.; Fernández de Valasco-Ruiz, M.; Barrales-Rienda, J. M. Macromol Chem Phys 2000, 201, 375.
23. Wunderlich, B. Macromolecular Physics, Vol. 1: Crystal Structure, Morphology, Defects; Academic Press: New York, 1973.
24. Hoffman, J. D.; Davis, G. T.; Lauritzen, J. I. In Treatise on Solid State Chemistry; Hannay, N. B., Ed.; Plenum: New York, 1976; p 497.
25. Burger, M. In: Free Boundary Problems; Colli, P., Ed.; Birkhaeuser: Basel, 2003; p 65.
26. Hoffman, J. D.; Miller, R. B. In Advanced Materials Research; Psaras, P. A.; Langford, H. D., Eds.; National Academy Press: Washington, DC, 1987; p 245.